Managing Smoke Risk from Wildland Fires: Northern California as a Case Study

Karina E. Chung[1], Tianjia Liu[2*], Makoto M. Kelp[3], Karn Vohra[4], Dana Skelly[5], Matthew C. Carroll[6], Joel Schwartz[7], and Loretta J. Mickley[1]

[1] John A. Paulson School of Engineering and Applied Sciences, Harvard University, Cambridge, MA, USA
[2] Department of Geography, University of British Columbia, Vancouver, BC, Canada
[3] Doerr School of Sustainability, Stanford University, Stanford, CA, USA
[4] School of Geography, Earth and Environmental Sciences, University of Birmingham, Birmingham, UK
[5] United States Department of Agriculture Forest Service, Portland, OR 97204, USA
[6] United States Department of Agriculture Forest Service, Bar Harbor, ME, USA
[7] T.H. Chan School of Public Health, Harvard University, Cambridge, MA, USA

*Corresponding author: Tianjia Liu (tianjia.liu@ubc.ca)

Abstract

Smoke fine particulate matter ($PM_{2.5}$) from increasing wildfires in the western United States threatens public health. While land managers often prioritize reducing wildfire risk in the wildland-urban interface, the impact on regional air quality from mitigating wildfire spread is less explored. We develop a framework to quantify wildfire contributions to smoke exposure and assess targeted land management strategies. This data-driven approach integrates fire emissions and smoke transport to generate a smoke risk index at 0.25°×0.25° resolution. We deploy the smoke risk index in an online tool, enabling stakeholders to analyze smoke risk under various scenarios of burned area, fuel consumption, and land management. Using Northern California as a case study, we estimate that in 2020, targeted land management in the 15 highest-risk areas (~3.5% of the total) could have reduced smoke exposure by 17.6%. However, most prescribed burns conducted from 2017-2020 did not overlap with these high-risk zones. Our framework also estimates excess deaths from smoke $PM_{2.5}$ exposure, attributing ~36,400 (95% CI: 25,400-47,200) deaths nationally due to western US fires in the year following the 2020 fire season. Our adaptable tool can incorporate higher-resolution datasets and help stakeholders prioritize fuel treatment and fire suppression to mitigate smoke exposure risks.

Keywords: Wildland fires, land management, health effects, smoke, $PM_{2.5}$

1. Introduction

In the western US, smoke fine particulate matter ($PM_{2.5}$) pollution from wildfires poses a large environmental threat to public health and threatens to undo decades of progress in air pollution reduction under the Clean Air Act (Burke et al., 2023; Jaffe et al., 2020). The long-range transport of smoke extends the impact of wildfires far beyond the immediate fire perimeter, with broad implications for air quality and public health. However, the potential smoke exposure from future wildfires is not typically taken into consideration when planning prescribed fires: the primary focus remains on addressing impacts directly within the path of wildfires (U. S. Department of Agriculture, 2023; U.S. EPA, 2021). Here, we present a smoke risk assessment tool that develops an array of emissions scenarios based on land-atmosphere variables. Our adaptable framework allows users to assess the most impactful locations from a public health perspective for the application of prescribed fires and fuel treatments in the western US.

$PM_{2.5}$ can penetrate deep into the lungs, leading to an array of health effects, including pulmonary disease, stroke, and premature death (e.g., Bell et al., 2014; Dockery et al., 1989; Yitshak-Sade et al., 2021). Vulnerable populations (Afrin and Garcia-Menendez, 2021; Kelp et al., 2023) and individuals with preexisting respiratory or cardiovascular conditions, most prevalent among elderly populations, are especially at risk (Faustini et al., 2013; Liu et al., 2017). Recent increases in wildfires in the western US stem from a combination of prolonged drought due to climate change, historical build-up of fuels from aggressive suppression efforts, and increased ignitions due to human population growth in the wildland-urban interface ("WUI") (Feng et al., 2024b, Guo et al., 2024; Williams et al., 2020). These compounding risks have made it difficult for nature to self-correct and require large-scale ecosystem restoration and management (Hessburg et al., 2015). Thus, state and federal agencies increasingly seek to expand the scope of prescribed burning and fuel treatments to minimize the impacts of large wildfires (California's strategic plan for expanding the use of beneficial fire, 2022).

The US Forest Service (USFS) and California Department of Forestry and Fire Protection (CAL FIRE) have plans to treat, with 40% through prescribed burning, one million acres per year in California as part of the Joint Stewardship Agreement (California's Wildfire and Forest Resilience Action Plan, 2021; Kramer et al., 2023). Current agency tools (e.g., BlueSky, HYSPLIT, HRRR-Smoke) used to assess likely prescribed fire emissions mostly focus on modeling overall smoke spread and pooling, and this analysis often occurs after burn locations are identified during land management planning (Ahmadov et al., 2017; Ferner and Meriam, 2022; Larkin et al., 2009). Developing a $PM_{2.5}$ smoke exposure tool is a data-intensive process, requiring both historical and projected fire emissions in addition to local and synoptic meteorological patterns that influence the transport of smoke into and out of different regions. Considering the large interannual variability in wildfire activity and the uncertainty in atmospheric transport of pollution, accurately quantifying and projecting smoke exposure at a fine spatial scale remains challenging.

Recent studies investigating historical wildfire activity in the WUS have focused on wildfire and smoke exposure trends (e.g., Abatzoglou and Williams, 2016; Burke et al., 2023; Childs et al., 2022; McClure and Jaffe, 2018; O'Dell et al., 2019), smoke transport (Barbero et al., 2014; Wu et al., 2012), and the health impacts of smoke exposure (e.g., Aguilera et al., 2021; Magzamen et al., 2021; Reid et al., 2016). To quantify the smoke fraction in surface $PM_{2.5}$, many of these studies designed statistical models relying on NOAA's Hazard Mapping System (HMS) smoke product of plumes digitized by analysts from satellite observations (Burke et al., 2023; Childs et al., 2022; O'Dell et al., 2021; Zhou et al., 2021). This approach, however, may incur large spatial biases as most smoke transported from the western US to the East is found to be aloft and does not affect surface air quality (Liu et al., 2024). Relatively few studies have employed physics and chemistry-based mechanistic models to connect fire emissions with meteorological transport to calculate population-weighted smoke exposure downwind of the fires (e.g., Kelp et al., 2023; Koplitz et al., 2016; Marlier et al., 2019; U.S. EPA, 2021). To our knowledge, there exist no studies adopting this framework to connect near-term fire emissions with land management scenarios for maximizing public health benefits in the western US.

In this study, we design the Smoke Management and Risk Tool: Fire-Land-Atmosphere Mapped Scenarios (SMRT-Flames) to assess smoke exposure across the western US and target areas where prescribed fires and other fire management approaches would yield the greatest benefit to air quality downwind. We use Northern California as a case study and extend the baseline framework used in Kelp et al. (2023) and Marlier et al. (2019). Our data-driven approach integrates (1) historic and near-term fire emissions related to land use, (2) meteorology-driven transport and deposition patterns of smoke to downwind regional population centers, and (3) resultant population-weighted exposure for a variety of land management scenarios. To evaluate our framework against other empirical approaches, we estimate the historical smoke concentrations and premature mortality attributable to fires across the western US. Our work aims to identify high smoke-risk areas for wildfire prevention, thereby reducing smoke $PM_{2.5}$ exposure downwind, especially among vulnerable populations.

2. Methods

Figure 1 shows a schematic workflow of our approach for SMRT-Flames. The baseline framework, taken from Kelp et al. (2023) and Marlier et al. (2019), consists of atmospheric transport (Section 2.1), historical fire emissions (Section 2.2), and calculation of smoke concentrations and related public health impacts (Section 2.3). Using Northern California as a case study, we modify this framework to calculate a smoke risk index and assess the potential impacts of various land management scenarios (Section 2.4). We define a "treatment zone" for land management and a "receptor" region for evaluating population-weighted smoke exposure. The treatment zone and receptor are decoupled in spatial extent, which makes it possible to assess the population-weighted exposure of multiple receptors (e.g., western US; southwestern US; Central Valley in California) given land management decisions in an input treatment zone (e.g., Northern California).

122

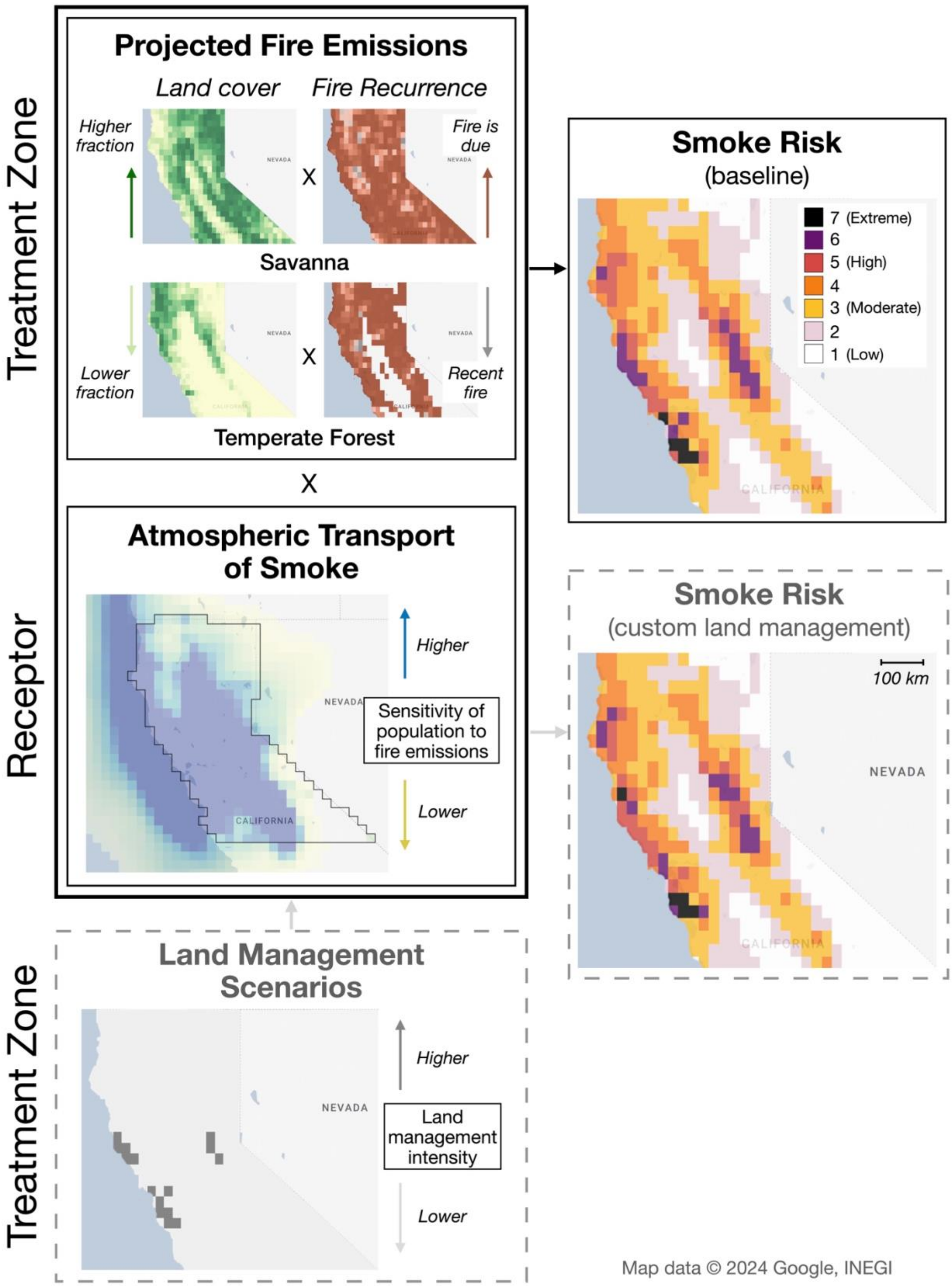
Treatment Zone
Projected Fire Emissions
Land cover
Fire Recurrence
Higher fraction
Fire is due
NEVADA
X
Savanna
Lower fraction
Recent fire
Temperate Forest
X
Receptor
Atmospheric Transport of Smoke
Higher
Sensitivity of population to fire emissions
Lower
CALIFORNIA
Treatment Zone
Land Management Scenarios
Higher
Land management intensity
Lower
Smoke Risk
(baseline)
7 (Extreme)
6
5 (High)
4
3 (Moderate)
2
1 (Low)
Smoke Risk
(custom land management)
100 km
Map data © 2024 Google, INEGI

Figure 1. Schematic workflow to generate the smoke risk index. The smoke risk index is a metric that highlights those grid cells where potential wildfires would pose the greatest smoke population-weighted smoke exposure downwind. The index is ranked by percentiles of smoke contribution within the treatment zone to the population-weighted average exposure across the specified receptor region. Inputs include projected fire emissions and atmospheric transport of smoke using sensitivity footprints from the adjoint of the GEOS-Chem model. The land cover fraction and recurrence interval, key components for calculating projected fire emissions, range from 0 to 1. Sensitivity footprints are driven by weather and represent the degree to which emissions in each grid cell contribute to overall smoke exposure in the receptor. An optional input is a land management scenario, which describes a historical or hypothetical prescribed fire or fuel treatment plan and ranges from 0 to 1. The background map data are from © 2024 Google, INEGI, rendered on Google Earth Engine Apps.

2.1 GEOS-Chem Adjoint and Meteorology

The adjoint of the GEOS-Chem (http://geos-chem.org) chemical transport model (CTM) calculates the sensitivity of population-weighted smoke exposure in specified receptor regions to wildfire emissions upwind. The adjoint considers the advection, convection, and deposition processes experienced by smoke plumes (Henze et al., 2007). Following the approach of previous studies (Kelp et al., 2023; Koplitz et al., 2016; Marlier et al., 2019), we use the adjoint of the GEOS-Chem v8-02-01 to quantify these source-receptor relationships. GEOS-Chem is driven by GEOS-FP assimilated meteorology from the NASA Global Modeling and Assimilation Office. Simulations have 0.25° × 0.3125° horizontal resolution over the nested North America domain (140°–40°W, 10°N–70°N). The method accounts for the spatiotemporal distribution of smoke plumes and generates monthly mean gridded sensitivities, referred to as adjoint sensitivities, from July to November—when fires are most active in the western U.S.—for the period 2016–2021, which includes both low and high fire years. We then resample the adjoint sensitivities to 0.25° × 0.25° spatial resolution to match the input fire emission database. The GEOS-Chem adjoint sensitivities also account for spatial variations in population within the receptor regions, which allows us to derive the population-weighted smoke exposure by multiplying these sensitivities with the estimated fire emissions (see Section 2.2). We define smoke as the primary $PM_{2.5}$ emitted by fires in the form of organic carbon (OC) and black carbon (BC) emissions (Wang et al., 2011). Following Koplitz et al. (2016), we multiply OC by a factor of 2.1 to account for aerosol aging (Turpin and Lim, 2001). The sum of the adjoint sensitivities multiplied by the fire emissions per grid cell yields the population-weighted smoke exposure in a receptor region for any fire emissions scenario, as the relationship between emissions at the source and smoke exposure at the receptor is assumed to be linear (Kim et al., 2015; Koplitz et al., 2016).

We divide the contiguous US into nine regional receptors as shown inset in Figure 2, following previous studies (Brey et al., 2018; O'Dell et al., 2021). We calculate the adjoint sensitivities given meteorological conditions from 2016 to 2021, yielding a set of monthly mean sensitivity maps spanning these six years. While meteorology is linked to droughts and the incidence of fires, this approach also allows us to capture much of the interannual variations in those meteorological processes, such as winds and precipitation, that affect smoke transport to the receptors. We assume that future interannual variability in transport is similar to that found during 2016-2021. To examine fires from 2003-2015, we match the meteorology of each year with that of one of the adjoint sensitivities from 2016-2021 based on the vapor pressure deficit (VPD) derived from ERA5-Land reanalysis meteorology (0.1° x 0.1°), averaged over the fire season and across the treatment zone (Hersbach et al., 2020). We then derive the projected smoke exposure contributions by multiplying the matching adjoint sensitivity with OC+BC emissions from the input year (Figures 1, S1).

2.2 Historical wildfire emissions

For historical wildfire emissions, we use the Global Fire Emissions Database version 4s (GFED4s) gridded at 0.25° × 0.25° spatial resolution in monthly timesteps (van der Werf et al., 2017). We use monthly GFED4s fire emissions in the western US receptor regions (Northwest, Southwest, and Rocky Mountains, abbreviated as NW, SW, and RM) from July-November 2003 to 2021. The fire emissions are based on observed relationships between the satellite-derived burned area from MODerate resolution Imaging Spectroradiometer (MODIS) observations and fuel consumption estimates from the Carnegie-Ames-Stanford Approach (CASA) biogeochemical model (Randerson et al., 2012; van der Werf et al., 2017). In GFED4s, fuel consumption is defined as the amount of biomass, coarse and fine litter, and soil organic matter consumed per unit area burned and is the product of fuel load and combustion completeness. Starting from 2017, GFED4s emissions are preliminary estimates, derived instead from the linear relationship between historical GFED4s emissions and MODIS active fire detections (van der Werf et al., 2017).

2.3 Calculating the health impacts from historical smoke $PM_{2.5}$ exposure

We assess the excess deaths attributable to smoke $PM_{2.5}$ from western US fires from 2003 to 2021 by using the parametric concentration-response function (CRF) detailed in Vodonos et al. (2018). Inputs in the CRF include the annual average of the population-weighted $PM_{2.5}$ with and without smoke contribution, population, and baseline mortality rates. The meta-analysis by Vodonos et al. (2018) includes 53 cohort studies that quantified the association between $PM_{2.5}$ exposure and increased mortality risk. The meta-analysis parametric model in Vodonos et al. (2018) approximates the long-term $PM_{2.5}$ mortality concentration response over a large range of $PM_{2.5}$ concentrations. Following Vohra et al. (2021), we calculate excess deaths as follows:

$$Excess\ deaths = BMR * p * AF \qquad \text{Eq. 1}$$

where *BMR* is the all-cause baseline mortality rate (number of deaths per 100,000 people), *p* is the total population over the age of 14 in the receptor region, and *AF* is the fraction of early deaths attributable to smoke $PM_{2.5}$ exposure. To evaluate excess mortality, we use the 2003-2019 state-level baseline mortality and population data from the Global Burden of Disease (GBD, 2019). For receptors that partially cover a state, we use the 2020 population counts from the 1-km Gridded Population of the World, version 4 (GPWv4.11) to approximate the fraction of the state population that lives within that receptor. We calculate the yearly receptor-level *BMR* in deaths per 100,000 people as the mean *BMR* in each state within the receptor weighted by the fraction of the receptor population living in that state, from 2003 to 2021. For 2020 and 2021, we use the *BMR* and population data from 2019 for our receptor-level *BMR* excess mortality findings. This likely led to underestimates in mortality for 2020-2021 due to compound effects from Covid-19 and wildfire smoke (Zhou et al., 2021). *AF* is calculated as follows:

$$AF = \frac{e^{(\bar{\beta} * x_{smoke})} - 1}{e^{(\bar{\beta} * x_{smoke})}} \qquad \text{Eq. 2}$$

$$x_{smoke} = x_{total} - x_{background} \qquad \text{Eq. 3}$$

$$\bar{\beta}(x) = \frac{1}{x_{smoke}} \int_{x_{background}}^{x_{total}} \beta(x)\, dx \qquad \text{Eq. 4}$$

where x is the mean annual population-weighted $PM_{2.5}$ concentration (in units of µg m^{-3}), x_{smoke} is the smoke $PM_{2.5}$, x_{total} is the total $PM_{2.5}$ from all sources, $x_{background}$ is non-smoke background $PM_{2.5}$, and $\bar{\beta}(x)$ is the mean long-term $PM_{2.5}$ mortality concentration-response from Vodonos et al. (2018), calculated as an average of $\beta(x)$ across a range of x from $x_{background}$ to x_{total}. To calculate x_{smoke}, we set the smoke $PM_{2.5}$ in non-fire months (January to June, December) to 0 µg m^{-3} and take the average across all months, an approach also taken by previous studies of smoke exposure (e.g., Koplitz et al., 2016; Marlier et al., 2019). To calculate $x_{background}$, we use surface $PM_{2.5}$ measurements from the US Environmental Protection Agency (EPA) air quality monitoring network. We approximate $x_{background}$ as the median $PM_{2.5}$ during non-fire months, averaged across monitors within the receptor region and weighted by the co-located GPWv4.11 population counts of the closest year (CIESIN, 2018).

Using the Vodonos et al. (2018) CRF, we estimate a 95% confidence interval (CI) for excess mortality estimates for each year from 2003 to 2021 based on calculated smoke $PM_{2.5}$ exposure from that year. The 95% CI reflects the uncertainty bounds only in the concentration response function and not in the BMR or population data. Given our focus on smoke exposure from wildfires ignited in the western US, we calculate the smoke $PM_{2.5}$ and health impacts for each region (Figure 2 inset) using only western US wildfire emissions. That is, we multiply all adjoint sensitivities for each receptor by the GFED4s emissions in grid cells only in the Northwest (NW), Rocky Mountains (RM), and Southwest (SW) regions in the western US. On a regional basis, we compare our modeled estimates of smoke exposure against a recent empirically derived dataset of wildfire smoke $PM_{2.5}$ from Childs et al. (2022).

2.4 Calculating smoke risk

The following subsections outline the key components of our wildfire smoke risk framework: land cover, burned area, and fuel consumption (Section 2.4.1); potential burned area and fire recurrence (Section 2.4.2); projected fire emissions and smoke exposure (Section 2.4.3); and smoke risk index (Section 2.4.4). We also deploy an online software tool that calculates the smoke risk under various scenarios of input burned area, fuel consumption, and land management (Section 2.4.5). Following Kelp et al. (2023), we select Northern California as a case study of interest in the tool, as it contains dense fuel loads and contributes a large proportion of population-weighted smoke exposure both in California and across the western US. Also, unlike chaparral or coastal shrub ecosystems elsewhere in the state, Northern California has been identified as a region that would benefit from wise prescribed fire management (California's strategic plan for expanding the use of beneficial fire, 2022).

2.4.1 Land cover, burned area, and fuel consumption

We use the 500-m annual MODIS land cover dataset (MCD12Q1) (Sulla-Menashe et al., 2019). Given their significant contribution to wildfire smoke in the western US, we focus only on regions identified as savanna (SAVA) or temperate forest (TEMF), two broad land cover types defined in GFED4s (Hessburg et al., 2015; van der Werf et al., 2017). We incorporate two types of dry matter (DM) emissions: historical 0.25° × 0.25° fire emissions estimates from GFED4s and potential emissions at the same horizontal resolution. Disaggregating DM emissions by land cover type enables accounting for differences in fuel consumption, emissions factors, and varying land management techniques.

To calculate fuel consumption rates, we relate DM emissions to burned area by using the historical relationship between GFED4s DM emissions and burned area from 2003-2016, aggregated during fire season months. This approach is computationally fast and can be generalized across wildland regions globally but lacks the regional specificity implemented in traditional U.S. fuel consumption models such as CONSUME (Prichard et al., 2014). We separately calculate fuel consumption rates for savanna and temperate forests. Because GFED4s provides only total burned area, we use the 500-m MODIS MCD12Q1 land cover product and MCD64A1 burned area product to calculate the fraction of GFED4s burned area attributed to savanna or temperate forest in each grid cell (Giglio et al., 2016; Sulla-Menashe et al., 2019). We use the weighted mean ("mean") and percentiles to consider the intrinsic variability within fuel consumption (fc): "low" (25th percentile), "median", and "high" (75th percentile) fuel consumption scenarios (Table 1). The mean SAVA fc is 2.18 kg m^{-2} (range: 0.68-4.19), and the mean TEMF fc is 11.66 kg m^{-2} (range: 9.42-17.18).

2.4.2 Potential burned area and fire recurrence

To estimate the potential burned area ahead of an upcoming fire season, we multiply the potential burned area by the fire recurrence coefficient, which represents the risk of a wildfire in each grid cell given the context of its fire history. The potential burned area is determined by user-defined scenarios specifying the percentage of "savanna" and "temperate forest" burned. Users may use historical burned area estimates to inform this input. As later discussed in Section 2.4.5, additional spatial layers, such as land management intensity, can further refine the potential burned area. The fire recurrence coefficient follows the principle that areas recently encountering wildfires are less likely to burn again. We use the Mean Fire Return Interval (MFRI) in the LANDFIRE 2016 Biophysical Settings (BPS) dataset to determine the frequency at which fires have historically occurred in each grid cell (La Puma, 2023). LANDFIRE is an interagency program that maps vegetation, fire, and fuel characteristics at 30-m resolution across the US. To determine the time elapsed since the most recent fire in each grid cell, we use burned area and recurrence interval estimates. We use the MODIS MCD64A1 burned area (500 m), supplemented by the Monitoring Trends in Burn Severity (MTBS) dataset of final fire perimeters derived from Landsat (30 m) and Sentinel-2 (10-20 m) imagery (Eidenshink et al., 2007; Giglio et al., 2018; Picotte et al., 2020). Since the MTBS record (from 1984) starts earlier than MODIS (from 2000), we use MTBS to supplement the MODIS fire history. The recurrence coefficient (rc) is calculated as follows:

$$t_{sincefire} = min[(t_0 - t_{MTBS}),\ (t_0 - t_{MCD64A1})] \quad \text{Eq. 5}$$

$$rc = \begin{cases} \frac{t_{sincefire}}{MFRI},\ t_{sincefire} < MFRI \\ 1,\ t_{sincefire} \geq MFRI \end{cases} \quad \text{Eq. 6}$$

where t_0 is the input emissions year, t_{MTBS} is the last year with a MTBS fire perimeter relative to t_0, $t_{MCD64A1}$ is the last year with MCD64A1 burned area relative to t_0, $t_{sincefire}$ is the number of years since the last fire, and $MFRI$ is the LANDFIRE MFRI. The rc is scaled to a range between 0 (low likelihood to burn, or recent burn) and 1 (high likelihood to burn, or fire is due).

2.4.3 Projected fire emissions and smoke exposure

We combine the potential burned area (BA), the corresponding fuel consumption level (fc), and the recurrence coefficient (rc) to calculate the projected dry matter emissions for each land cover type as follows:

$$DM = DM_{SAVA} + DM_{TEMF} \quad \text{Eq. 7}$$

$$DM_{SAVA} = fc_{SAVA} * BA_{SAVA} * rc_{SAVA} \quad \text{Eq. 8}$$

$$DM_{TEMF} = fc_{TEMF} * BA_{TEMF} * rc_{TEMF} \quad \text{Eq. 9}$$

For each grid cell, we project the fire emissions for grid cell (E), or the OC+BC emissions, for land-cover specific DM emissions (DM_{SAVA} and DM_{TEMF}). We calculate fire emissions using the GFED4s dry matter emissions (DM) and Akagi et al., (2011) emissions factors (EF) as follows:

$$E = DM_{SAVA} * EF_{SAVA} + DM_{TEMF} * EF_{TEMF} \quad \text{Eq. 10}$$

Our overall smoke risk assessment metric, $PM_{2.5}(proj)$, in units of μg m^{-3}, projects the contribution of each grid cell to the population-weighted smoke $PM_{2.5}$ of the receptor during the fire season months (July to November) in a given input year. To calculate this projection, we multiply the projected fire emissions E, in units of kg m^{-2}, by the GEOS-Chem adjoint sensitivity (S), in units of (μg m^{-3})/(kg m^{-2}), as follows:

$$PM_{2.5}(proj) = E \times S \qquad \text{Eq. 11}$$

2.4.4 Smoke risk index conversion

We consolidate the projected population-weighted smoke exposure for each grid cell into a smoke risk index to help land managers identify regions that pose relatively greater smoke risk to populations downwind. Our risk map groups grid cells into six categories of relative risk, based on the following percentile cutoffs: 0-25% (Level 1, "little to no risk"), 25-50% (Level 2, "low risk"), 50-75% (Level 3, "moderate-low risk"), 75-90% ("moderate risk"), 90-95% (Level 5, "high risk"), 95-99% (Level 6, "very high risk"), and over 99% (Level 7, "extreme risk"). Due to the heavy-tailed nature of the distribution of smoke $PM_{2.5}$ exposure across Northern California, we use the 99th percentile cutoff to distinguish very high risk from extreme risk. We focus on the top 15 grid cells, corresponding to ~3.5% of total area.

2.4.5 Google Earth Engine online tool

We deploy the smoke risk index and health analysis in a Google Earth Engine online tool, SMRT-Flames (https://smoke-policy-tool.projects.earthengine.app/view/smrt-flames), to support end users such as land and air quality managers (Figure S4). Google Earth Engine is a cloud-based platform that supports geospatial analysis, online visualization, and web app deployment through Earth Engine Apps (Gorelick et al., 2017). The tool enables end users to estimate the relative population-weighted smoke risk given an input treatment zone, receptor, fire emissions year, and meteorology year. We include fire emissions from 2003 to 2021 and meteorological scenarios from the GEOS-Chem adjoint from 2016 to 2021. Here, we implement Northern California as the input treatment zone for a case study.

First, the tool enables users to select a treatment zone and receptor, which are decoupled in spatial extent. For example, Northern California can be selected as the treatment zone, and Central Valley as the receptor. The fire emissions year and the meteorology year can be varied to examine potential differences in smoke risk attributable to different weather patterns. Second, users can adjust the fuel consumption rate of a potential wildfire or prescribed fire treatment, and the fraction of area burned for both savannas and temperate forests based on historical burn fractions or existing land management plans for the two land cover types. Finally, users can choose the intensity of a land management treatment based on (1) a "targeted" scenario of high smoke risk areas identified by the smoke risk index or (2) a "variable" scenario based on historical or planned prescribed fires and fuel treatments. While the targeted scenario applies a uniform land management intensity (LMI) to a select number of grid cells with the highest smoke risk, the variable scenario allows the LMI to vary by grid cell according to user input. The scenarios allow users to identify priority areas for reducing smoke exposure given recent land management activities and acts as a dampening factor on fire emissions, similar to the recurrence interval.

As an example, we use prescribed burns recorded in the National Fire Plan Operations and Reporting System (NFPORS), used by the U.S. Department of Agriculture and Department of the Interior, and by CAL FIRE's Fire and Resource Assessment Program (FRAP) as a proxy for land management intensity from December 2017 to June 2020, or the time period between the end of the 2017 fire season and just prior to the 2020 fire season. We remove NFPORS records that are likely duplicates by spatially filtering NFPORS coordinates within FRAP polygons. We make two assumptions: (1) that areas where prescribed fires occur have higher resource allocation and land management intensity, making wildfires in these areas easier to control and extinguish, and (2) that prescribed burns moderate future wildfires in a grid cell and decrease fire severity, leading to lower fire emissions (Cansler et al., 2022). We aggregate the total area of prescribed fires at 0.25° x 0.25° resolution and scale LMI levels between 0 and 1, where 0 is no land management and 1 is no fire emissions due to aggressive treatment. For intermediate LMI values, we create bins based on the relative distribution of treatment sizes found in NFPORS and FRAP: < 100 acres = 0.05, 100-500 acres = 0.1, 500-1000 acres = 0.2, 1000-1500 acres = 0.3, 1500-2000 acres = 0.4, and > 2000 acres = 0.5. In the default scenario, the tool calculates the impact of a risk-optimized scenario with a high LMI of 0.5 applied to the top 15 at-risk grid cells, equivalent to 30,000 acres treated (Table 1).

In addition, we test the impact of several hypothetical land management scenarios on overall population exposure. In line with recent state and federal prescribed fire activities and plans in California (California's strategic plan for expanding the use of beneficial fire, 2022), we test two additional risk-optimized scenarios of 100,000 acres treated annually using prescribed fire in Northern California. In the first scenario, 100 grid cells are treated with a medium LMI of 0.25, and in the second scenario, 50 grid cells are treated with a high LMI of 0.5. The user input layer is flexible to further adjustments to the land management intensity levels, especially as future studies aim to quantify the efficacy of prescribed fires and fuel treatments for reducing wildfire occurrence, fire spread, and burn severity (Kelp et al., 2024). Other adjustments can include using estimates of planned resource allocation due to high tree mortality (Stephens et al., 2018) or wildfire suppression difficulty (Silva et al., 2020).

Table 1. **Land management scenarios.** Detailed definitions of each historical and hypothetical land management scenario for Northern California in 2020.

Scenario	**Type**	**Description**	**Area Treated** (acres)
Baseline		No future treatments are applied	0
NFPORS + FRAP[1]	Historical	Combined federal and state prescribed burns from NFPORS and FRAP from December 2017 to June 2020	285,955
Risk-optimized (15, High)	Hypothetical	15 highest-risk grid cells (according to the smoke risk index), treated with LMI = 0.5	30,000
Risk-optimized, (100, Medium)	Hypothetical	100 highest-risk grid cells, treated with LMI = 0.25 (1,000 acres per grid cell)	100,000

Risk-optimized, (50, High)	Hypothetical	50 highest-risk grid cells, treated with LMI = 0.5 (2,000 acres per grid cell)	100,000

[1] NFPORS is the National Fire Plan Operations and Reporting System and FRAP is the Fire and Resource Assessment Program. NFPORS is operated at the federal level by the US Forest Service and FRAP includes state-level efforts with CAL FIRE involvement.

3. Results and Discussion

Following Koplitz et al. (2016), we first quantify the annual health impacts of smoke $PM_{2.5}$ originating from the western US from 2003 to 2021. We then demonstrate how an extended framework can be used as a land management tool using Northern California as a case study (Figure 1).

3.1 Annual health impacts from western US smoke

We find that air pollution-related deaths from western US wildfire smoke predominantly affect populations aged 14 years and above in the western US, with little influence east of the Rocky Mountains. Figure 2 shows the variation in excess mortality attributable to smoke $PM_{2.5}$ from western US fires from 2003 to 2021. The calculated mortalities reflect interannual variability in wildfire activity with several recent extreme wildfire seasons since 2017. The peak occurs in the 12-month aftermath of the 2020 fire season during which we find that excess mortality due to smoke from western US fires reached 34,900 deaths (95% CI: 24,500-45,000) in western US receptors alone, with 1500 (95% CI: 900-2,200) deaths east of the Rockies. From 2003 to 2021, our mean estimates show that 94% of all mortalities from western US wildfires occurred locally, whereas 6% occurred east of the Rocky Mountains. Although smoke from prescribed fires in the eastern US is an air quality concern (Afrin and Garcia-Menendez, 2021) and wildfire activity may increase in the southeastern US in the coming decades (Donovan et al., 2023), we find little evidence that wildfire smoke emanating from the western US occurred at levels that affected the health of populations in the eastern US from 2003 to 2021 (Figure 2). However, our study does not consider wildfire smoke originating outside of the U.S. Canada, for example, has been shown to impact communities in the Midwest and East Coast (K. Chen et al., 2023; Ford et al., 2018; Yu et al., 2024). Variability in annual meteorology had a small effect on annual smoke concentrations and by extension, public health impacts (Figure S1). The coefficient of variation, or the standard deviation divided by the mean, of annual smoke $PM_{2.5}$ ranges from 9-27% under the meteorological range of the 2016-2021 adjoint sensitivities.

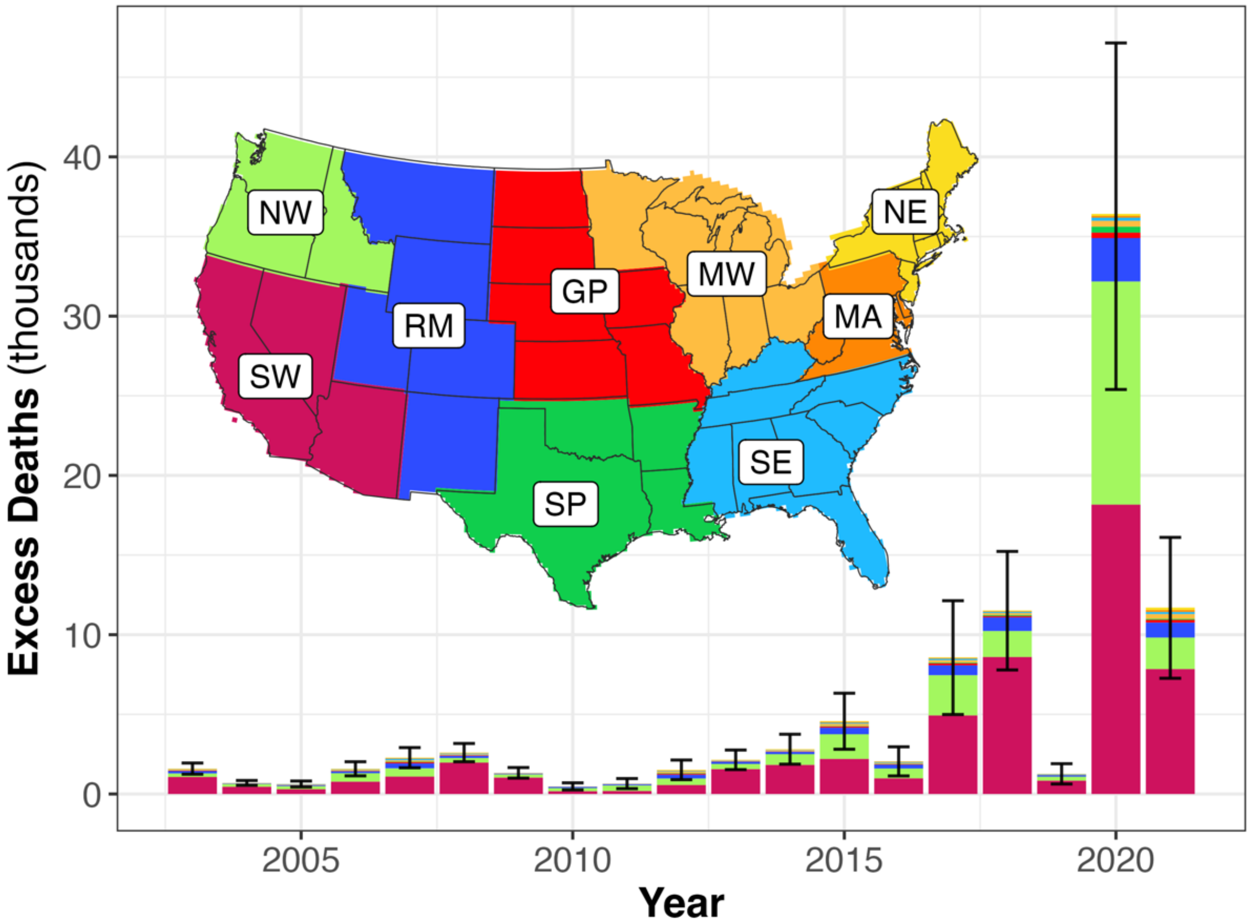

Figure 2. Excess deaths attributable to smoke $PM_{2.5}$ exposure across the contiguous US from western US fires. The annual excess mortalities from 2003 to 2021 are separated by region, or receptor, across CONUS. The inset map defines the receptor regions, following O'Dell et al. (2021): Northwest (NW), Southwest (SW), Rocky Mountains (RM), Great Plains (GP), Southern Plains (SP), Midwest (MW), Mid Atlantic (MA), Northeast (NE), and Southeast (SE). Error bars correspond to the 95% confidence interval of total excess deaths across CONUS.

The calculated smoke $PM_{2.5}$ and health impacts presented here show differences compared to datasets that rely on the unequal distribution of surface $PM_{2.5}$ monitoring networks. Figure S2 compares our CTM-based excess mortality estimates from smoke exposure in the western US with those derived from a combination of surface $PM_{2.5}$ measurements and HMS smoke plumes in Childs et al. (2022). In low fire years (e.g., 2006-2016), our estimates of excess mortality attributable to smoke exposure agree well with Childs et al. (2022). For 2020, however, the Childs et al. (2022) dataset of smoke $PM_{2.5}$ yields approximately 21,700 excess deaths (95% CI: 14,000-29,200) in the western US, 40% less than our higher mean estimate of approximately 36,400 deaths (95% CI: 25,400-47,200). Given the use of the same CRF for excess deaths calculations in both datasets, we attribute this discrepancy to differences in approaches in estimating wildfire smoke $PM_{2.5}$ exposure for the 2020 fire season. For example, as discussed in Qiu et al. (2024), possible uncertainties for our CTM-based approach arise from the GFED4s fire emissions estimates, GEOS-Chem boundary layer mixing, and smoke injection heights, which may have led to overestimation of smoke $PM_{2.5}$ during the intense 2020 wildfire season. In contrast, the machine learning-based approach of Childs et al. (2022) may underestimate extreme smoke $PM_{2.5}$ values or may struggle to represent smoke transport in data-sparse areas where EPA stations are lacking, or HMS smoke day definitions may be unreliable.

3.2 Smoke risk and land management case study in Northern California

Excess deaths in Northern California comprise about a third of the total $PM_{2.5}$-attributable mortality to western US wildfires in 2020. Due to the co-occurrence of high fire activity and smoke exposure, we focus on Northern California for our case study. Our framework identifies locations with the greatest contribution to the overall risk of smoke exposure and the associated adverse health effects across all grid cells in Northern California. Figure 3 shows the projected smoke risk index for Northern California in 2020 for the baseline scenario, which does not consider any historical or hypothetical land management scenarios. We use the historical average percent of total savanna (5.85%), and temperate forest (9.33%) burned to define the baseline emission scenario for the Northern California treatment zone in 2020.

We find that the 15 grid cells with the highest smoke risk to downwind populations are found in heavily forested regions and within the WUI surrounding San Francisco, San Jose, and Sacramento (Figure 3a). As seen in 2020, the occurrence of several large wildfires near the San Francisco and San Jose WUI regions, including the CZU (86,509 acres) and SCU Lightning Complex (396,624 acres), underscores the potential fire and smoke risk near dense urban centers. The priority smoke risk areas may shift if specifying other receptors. For example, in the Central Valley receptor the priority grid cells shift away from the San Francisco and San Jose WUI region to forested areas northeast of Sacramento (Figure 3b). These results underscore the WUI as a high-risk area for population-weighted smoke exposure, reinforcing its importance in prescribed fire management policies across the western U.S. While protecting communities in the WUI remains a heightened policy focus area, recent work has shown that land management within these areas has been less effective at reducing future burn severity and smoke emissions compared to treatments outside the WUI (Kelp et al., 2024). These findings emphasize the need to reassess current strategies and develop more effective interventions to address the unique challenges of WUI management while enhancing smoke risk reduction.

We find that the smoke risk index is sensitive to the percent burned in savannas relative to that in temperate forest areas, signifying the importance of land cover and fuel composition. The smoke risk index is not intended to predict the exact locations of fires, whose ignitions are difficult to pinpoint and vary significantly from year to year (Figure S3). On a longer timescale, however, we find that wildfires do tend to occur within the moderate-to-extreme smoke risk areas, and our fire recurrence coefficient acts as a constraint on potential wildfire locations. The recurrence coefficient shows a large fire deficit in the treatment zone with values close or equal to 1, underscoring a need for prioritizing future treatments with maximal co-benefits in those areas (Figure 1).

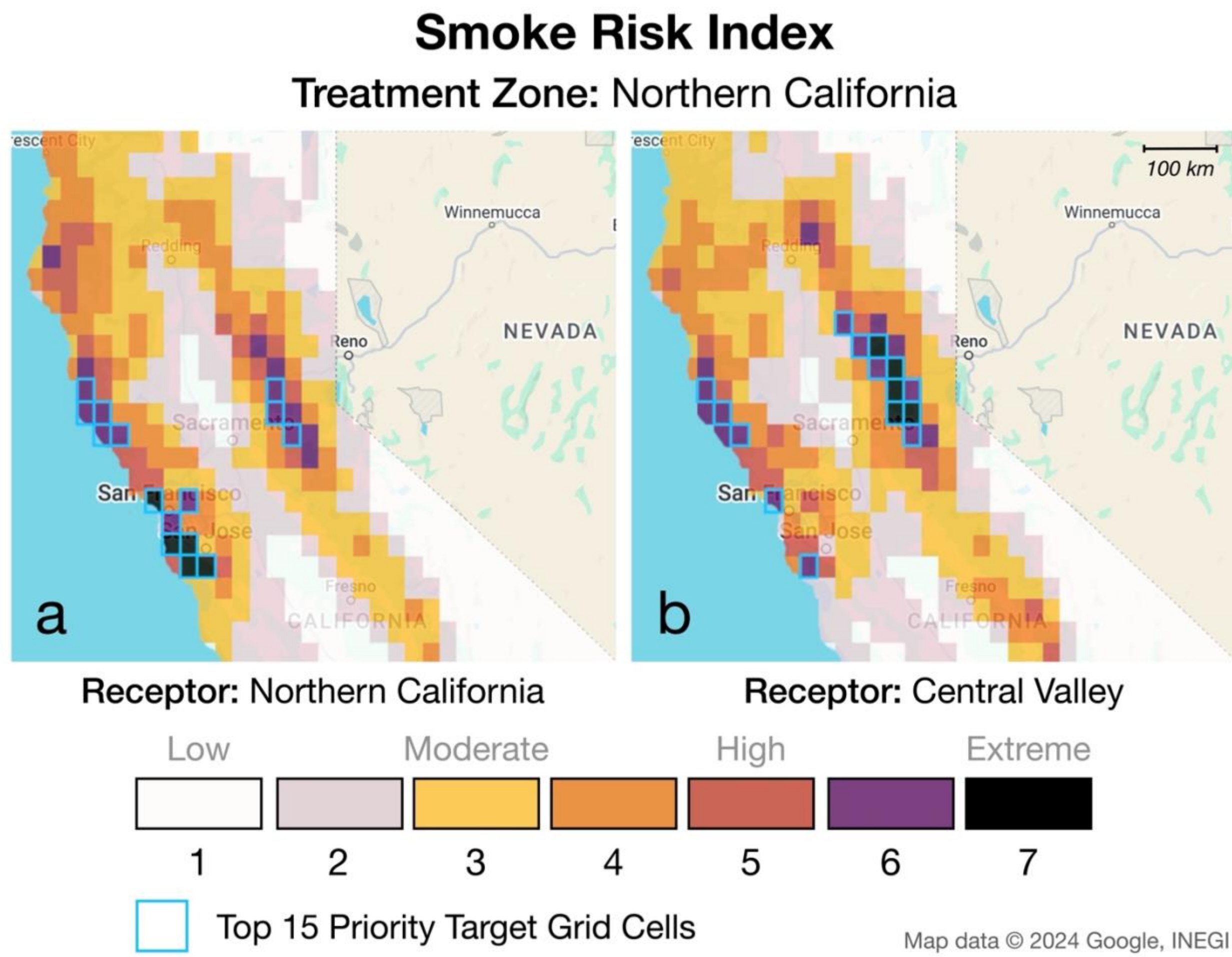

Figure 3. **Smoke risk index for the Northern California treatment zone in 2020.** Darker colors indicate those grid cells where potential wildfires would pose the most risk for population-weighted smoke exposure in the two receptors, (a) Northern California and (b) Central Valley. Blue boxes indicate the 15 priority target grid cells that pose the greatest smoke exposure risk to these regional populations. Results are shown for the baseline scenario, which assumes that 5.85% of the total savanna area and 9.33% of the total temperate forest area burn with mean fuel consumption in Northern California**.** The background map data are from © 2024 Google, INEGI, rendered on Google Earth Engine Apps.

Next, we examine the potential reduction in population-weighted smoke exposure from the baseline scenario (Figure 3), in response to four simulated land management scenarios (Table 1, Figure 4). These four scenarios represent a (1) risk-optimized land management approach that applies a high LMI (0.5) to the top 15 priority grid cells with the largest potential impact on population-weighted smoke exposure in Northern California, (2) historical state and federal prescribed burns in the two years prior to the 2020 fire season, and two additional risk-optimized approaches aligned with the CAL FIRE land management near-term target of 100,000 acres treated at (3) medium LMI (0.25) for 100 grid cells and (4) high LMI (0.5) for 50 grid cells.

Figure 4 illustrates the land management intensity defined for the four scenarios and shows the effect of each land management strategy on the population-weighted smoke exposure in Northern California. Based on an LMI of 0.5, or equivalent to a 50% reduction in fire emissions by treating 2000 acres, we find that the treatment of the 15 high-risk areas under a risk-optimized approach would have reduced smoke $PM_{2.5}$ exposure in Northern California by 17.6%. In contrast, state and federal prescribed fire treatments from December 2017 to June 2020 mostly occurred outside the 15 high-risk areas in the historical land management scenario, dampening the efficacy of smoke risk reduction to 14.2%. For a target of 100,000 acres treated, the high-intensity CAL FIRE scenario shows a higher potential (32.2%) to reduce smoke exposure compared to the medium-intensity CAL FIRE scenario (20.6%). This finding aligns with previous studies (Deak et al., 2024; Kelp et al., 2023) that suggest fewer, larger, and more intense prescribed fire treatments may be more efficient and effective than numerous smaller ones.

Overall, our four scenarios illustrate the potential benefits of targeted, preventative land management efforts. Further adjustments can be applied to balance the LMI and spatial extent of treatments based on cost and feasibility. For example, a tiered system could be implemented that applies different land management intensity designations according to smoke risk. In addition, future work is needed to assess land management intensity, which intends to capture the efficacy of fuel treatments, suppression difficulty, and proactive community efforts to reduce wildfire risk. Establishing more accurate, quantitative relationships between these local to federal-level efforts and land management intensity is critical for improving estimates of smoke risk.

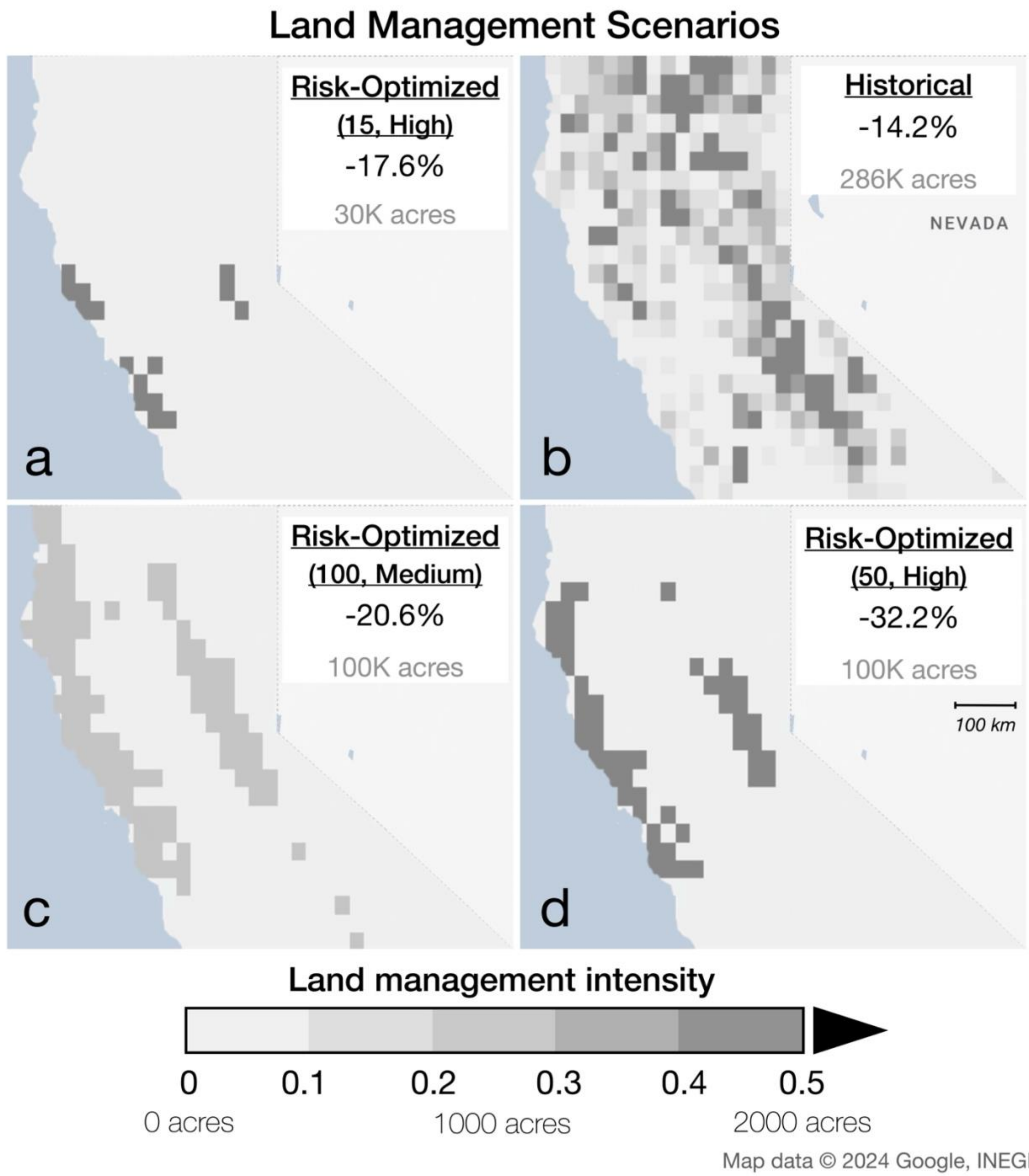

Figure 4. **Four land management scenarios for Northern California.** The panels show the land management intensity (LMI), defined in Table 1, for these scenarios: (a) Risk-Optimized, in which the top 15 highest-risk grid cells are treated with a LMI of 0.5 (2000 acres per grid cell), (b) Historical, which includes the prescribed burns from NFPORS and FRAP from December 2017 to June 2020, and two additional Risk-Optimized scenarios based on a prescribed burn target of 100,000 acres, in which (c) the 100 highest-risk grid cells are treated with an LMI of 0.25 (1000 acres per grid cell), and (d) the 50 highest-risk grid cells treated an LMI of 0.5 (2000 acres per grid cell). Text inset shows the reduction in population-weighted smoke exposure in Northern

California, compared to the baseline scenario in Figure 3. The background map data are from © 2024 Google, INEGI, rendered on Google Earth Engine Apps.

3.3 Comparison to existing wildfire smoke tools

Current agency tools for modeling and projecting wildfire smoke, such as BlueSky (USFS) and HRRR-Smoke (NOAA), primarily focus on short-term predictions or often emphasize immediate impacts on air quality (Ahmadov et al., 2017; Larkin et al., 2009). BlueSky integrates a variety of fire behavior models with emissions and dispersion models to simulate smoke trajectories, providing users with estimates of near-term air quality impacts from wildfires or prescribed burns. HRRR-Smoke is a real-time modeling system embedded within the High-Resolution Rapid Refresh (HRRR) weather model. It can provide high-resolution, near-term forecasts of smoke dispersion and its impacts on air quality and visibility. However, both BlueSky and HRRR-Smoke focus primarily on short-term meteorological and fire behavior-driven predictions and does not integrate longer-term, seasonal analyses of smoke exposure trends or land management practices.

In contrast to these approaches, our tool, SMRT-Flames, extends these models by focusing on long-term, population-weighted exposure to smoke $PM_{2.5}$. By incorporating historical fire activity, historical and projected fire emissions data, and physics-driven meteorological transport of smoke, our approach evaluates the efficacy of prescribed burning and land management strategies over time. SMRT-Flames allows for strategic planning aimed at minimizing cumulative public health impacts while balancing the ecological and fire mitigation costs and benefits of prescribed fire. Unlike many smoke models, our framework quantifies the effects of proactive land management interventions to understand our ability to reduce smoke burdens in vulnerable communities while supporting sustainable fire management practices.

3.4 Limitations

Limitations in our framework can be traced to uncertainty in fire emissions, atmospheric transport, and excess mortality estimates. We rely on the GFED4s fire emissions inventory, which uses a linear relationship between active fire detections and dry matter emissions after 2016 (van der Werf et al., 2017). The forthcoming GFED5 uses updated burned area estimates by incorporating adjustment factors based on Landsat and Sentinel-2, which have a higher spatial resolution (10-30 m) than MODIS (500 m-1 km) (Y. Chen et al., 2023). Low-intensity fires or prolonged cloud and haze coverage may contribute to underestimates of fire emissions. Another caveat is that GFED4s does not include plume injection information or fire-specific diurnal cycles, which are important for characterizing smoke transport for severe wildfires in CTMs such as GEOS-Chem (Feng et al., 2024a; Liu et al., 2024; Qiu et al., 2024). Qiu et al. (2024) show that machine learning-based approaches tend to outperform CTMs in the western US when compared to surface monitor observations of $PM_{2.5}$. However, only the CTM approach using the GEOS-Chem adjoint enables our framework for modifying historical or projected fire emissions based on land management scenarios. Another limitation is that we implemented GEOS-Chem adjoint sensitivities for only 2016 through 2021; meteorological conditions in future years may fall outside of this range, and seasonal climate outlooks prior to the fire season may not accurately represent the upcoming fire weather conditions. Additionally, improving the temporal scale of SMRT-Flames from seasonal to monthly or weekly could support customization for short-term variations in fuel conditions and burn windows. Furthermore, the CRFs used to estimate excess mortality from smoke concentrations continue to be updated with new cohort studies (Connolly et al., 2024; Vodonos et al., 2018; Vohra et al., 2021). The Vodonos et al. (2018) CRF used in this study does not account for potentially higher $PM_{2.5}$ toxicity from smoke versus other sectors, or smoke from wildfires versus prescribed fires (Tuet et al., 2019; Verma et al., 2015). The 95% CI for our premature mortality estimates considers uncertainties only in the CRF and not in the BMRs and population datasets. Compound effects from heatwaves or pandemics may also complicate excess mortality estimates (Zhou et al., 2021). For land management, the lack of prescribed fire activity in the western US in recent decades means that its potential for reducing future wildfire severity and spread is currently not well-quantified, let alone for different treatment types (e.g. broadcast burns versus pile burns) or additional fuel reduction methods (e.g., thinning). Finally, our study does not explore the tradeoffs in smoke exposure for increasing prescribed burns versus wildfires (Kelp et al., 2024; Schollaert et al., 2024; U.S. EPA, 2021).

4. Conclusion

Increasing smoke exposure from wildfires in the western US underscores the urgency of optimizing land management to account for longer-term health impacts. We estimate that the 2020 fire season in the western US led to approximately 36,400 excess deaths (95% CI: 25,400-47,200) across the contiguous US, with 96% of deaths occurring locally within the western US. Despite the significant health burden of smoke exposure, there is an opportunity to improve the ability of land managers to assess this risk when planning prescribed fires or other fuel treatments. To address this gap, we designed a data-driven framework to estimate historical and projected smoke risk for populations downwind of wildfires, including those living many kilometers away from the source region. We integrated the framework into an online tool that allows users to modify input parameters, such as meteorology, fuel consumption, and land management intensity. As a case study, we deployed this framework in Northern California to simulate the impact of land management scenarios on excess mortality from smoke exposure in downwind regions. We found that prior prescribed fires from December 2017 to June 2020 occurred mostly outside the 15 highest-risk areas identified by the tool. Additionally, we tested a target of 100,000 acres burned using prescribed fire in Northern California per year and find that a “high” intensity scenario is more effective at reducing smoke exposure than a “medium” intensity scenario, in which double the area is treated at half the intensity (-32.2% versus -20.6%). This result highlights the potential efficacy and higher efficiency of targeted preventative efforts. Our results also indicate that the WUI remains a high-risk area for smoke exposure, yet recent studies show that current land management efforts in these areas have been less effective at reducing future burn severity and smoke emissions than treatments outside the WUI. Our framework is flexible and can integrate additional on-the-ground information, such as prescribed burn and fuel treatment plans, as well as more detailed land cover and fuel classifications. By incorporating future smoke risk into land management planning, policymakers and land managers can enhance public health protection beyond the immediate fire zone.

Acknowledgements

This study was supported by the NOAA Climate Program Office's Modeling, Analysis, Predictions, and Projections Program (MAPP), Grant NA22OAR4310140. K. Chung acknowledges support from the Harvard College Research Program (HCRP). T. Liu and M. Kelp acknowledge support from the NOAA Climate and Global Change Postdoctoral Fellowship Program, administered by UCAR's Cooperative Programs for the Advancement of Earth System Science (CPAESS) under the NOAA Science Collaboration Program award NA21OAR4310383. We thank Len Nielson for helpful discussions regarding this work.

Data Availability

The Google Earth Engine online tool (SMRT-Flames) is available at: https://smoke-policy-tool.projects.earthengine.app/view/smrt-flames. All data used in this study are freely available. MODIS and GPW data are distributed by the NASA Earthdata platform (https://earthdata.nasa.gov/). LANDFIRE (https://landfire.gov/), MTBS (https://mtbs.gov/), and GFED4s (https://www.globalfiredata.org/) data were retrieved online from the data provider websites. Station $PM_{2.5}$ data from the US EPA are archived online (https://www.epa.gov/outdoor-air-quality-data/). GBD were retrieved from IHME (https://vizhub.healthdata.org/gbd-results/).

References

Abatzoglou, J.T., Williams, A.P., 2016. Impact of anthropogenic climate change on wildfire across western US forests. PNAS 113, 11770–11775. https://doi.org/10.1073/pnas.1607171113

Afrin, S., Garcia-Menendez, F., 2021. Potential impacts of prescribed fire smoke on public health and socially vulnerable populations in a Southeastern U.S. state. Science of The Total Environment 794, 148712. https://doi.org/10.1016/j.scitotenv.2021.148712

Aguilera, R., Corringham, T., Gershunov, A., Benmarhnia, T., 2021. Wildfire smoke impacts respiratory health more than fine particles from other sources: observational evidence from Southern California. Nat Commun 12, 1493. https://doi.org/10.1038/s41467-021-21708-0

Ahmadov, R., Grell, G., James, E., Csiszar, I., Tsidulko, M., Pierce, B., McKeen, S., Benjamin, S., Alexander, C., Pereira, G., Freitas, S., Goldberg, M., 2017. Using VIIRS fire radiative power data to simulate biomass burning emissions, plume rise and smoke transport in a real-time air quality modeling system, in: 2017 IEEE International Geoscience and

Remote Sensing Symposium (IGARSS). Presented at the 2017 IEEE International Geoscience and Remote Sensing Symposium (IGARSS), pp. 2806–2808. https://doi.org/10.1109/IGARSS.2017.8127581

Akagi, S.K., Yokelson, R.J., Wiedinmyer, C., Alvarado, M.J., Reid, J.S., Karl, T., Crounse, J.D., Wennberg, P.O., 2011. Emission factors for open and domestic biomass burning for use in atmospheric models. Atmospheric Chemistry and Physics 11, 4039–4072. https://doi.org/10.5194/acp-11-4039-2011

Barbero, R., Abatzoglou, J.T., Steel, E.A., Larkin, N.K., 2014. Modeling very large-fire occurrences over the continental United States from weather and climate forcing. Environ. Res. Lett. 9, 124009. https://doi.org/10.1088/1748-9326/9/12/124009

Bell, M.L., Ebisu, K., Leaderer, B.P., Gent, J.F., Lee, H.J., Koutrakis, P., Wang, Y., Dominici, F., Peng, R.D., 2014. Associations of PM2.5 Constituents and Sources with Hospital Admissions: Analysis of Four Counties in Connecticut and Massachusetts (USA) for Persons ≥ 65 Years of Age. Environmental Health Perspectives 122, 138–144. https://doi.org/10.1289/ehp.1306656

Brey, S.J., Barnes, E.A., Pierce, J.R., Wiedinmyer, C., Fischer, E.V., 2018. Environmental Conditions, Ignition Type, and Air Quality Impacts of Wildfires in the Southeastern and Western United States. Earth’s Future 6, 1442–1456. https://doi.org/10.1029/2018EF000972

Burke, M., Childs, M.L., de la Cuesta, B., Qiu, M., Li, J., Gould, C.F., Heft-Neal, S., Wara, M., 2023. The contribution of wildfire to PM2.5 trends in the USA. Nature 622, 761–766. https://doi.org/10.1038/s41586-023-06522-6

California’s strategic plan for expanding the use of beneficial fire. 2022. Retrieved from https://wildfiretaskforce.org/wp-content/uploads/2022/05/californias-strategic-plan-for-expanding-the-use-of-beneficial-fire.pdf

California’s Wildfire and Forest Resilience Action Plan: Recommendations of the Governor’s Forest Management Task Force, 2021.

Cansler, C.A., Kane, V.R., Hessburg, P.F., Kane, J.T., Jeronimo, S.M.A., Lutz, J.A., Povak, N.A., Churchill, D.J., Larson, A.J., 2022. Previous wildfires and management treatments moderate subsequent fire severity. Forest Ecology and Management 504, 119764. https://doi.org/10.1016/j.foreco.2021.119764

Chen, K., Ma, Y., Bell, M.L., Yang, W., 2023. Canadian Wildfire Smoke and Asthma Syndrome Emergency Department Visits in New York City. JAMA 330, 1385–1387. https://doi.org/10.1001/jama.2023.18768

Chen, Y., Hall, J., van Wees, D., Andela, N., Hantson, S., Giglio, L., van der Werf, G.R., Morton, D.C., Randerson, J.T., 2023. Multi-decadal trends and variability in burned area from the fifth version of the Global Fire Emissions Database (GFED5). Earth System Science Data 15, 5227–5259. https://doi.org/10.5194/essd-15-5227-2023

Childs, M.L., Li, J., Wen, J., Heft-Neal, S., Driscoll, A., Wang, S., Gould, C.F., Qiu, M., Burney, J., Burke, M., 2022. Daily Local-Level Estimates of Ambient Wildfire Smoke PM2.5 for the Contiguous US. Environ. Sci. Technol. https://doi.org/10.1021/acs.est.2c02934

Center for International Earth Science Information Network - CIESIN - Columbia University. 2018. Gridded Population of the World, Version 4 (GPWv4): Population Count Adjusted to Match 2015 Revision of UN WPP Country Totals, Revision 11. Palisades, NY: NASA

Socioeconomic Data and Applications Center (SEDAC). https://doi.org/10.7927/H4PN93PB.

Connolly, R., Marlier, M.E., Garcia-Gonzales, D.A., Wilkins, J., Su, J., Bekker, C., Jung, J., Bonilla, E., Burnett, R.T., Zhu, Y., Jerrett, M., 2024. Mortality attributable to PM2.5 from wildland fires in California from 2008 to 2018. Science Advances 10, eadl1252. https://doi.org/10.1126/sciadv.adl1252

Deak, A. L., Lucash, M. S., Coughlan, M. R., Weiss, S., & Silva, L. C. R. (2024). Prescribed fire placement matters more than increasing frequency and extent in a simulated Pacific Northwest landscape. Ecosphere, 15(4), e4827. https://doi.org/10.1002/ecs2.4827

Dockery, D.W., Speizer, F.E., Stram, D.O., Ware, J.H., Spengler, J.D., Ferris, B.G., 1989. Effects of Inhalable Particles on Respiratory Health of Children. Am Rev Respir Dis 139, 587–594. https://doi.org/10.1164/ajrccm/139.3.587

Donovan, V.M., Crandall, R., Fill, J., Wonkka, C.L., 2023. Increasing Large Wildfire in the Eastern United States. Geophysical Research Letters 50, e2023GL107051. https://doi.org/10.1029/2023GL107051

Eidenshink, J., Schwind, B., Brewer, K., Zhu, Z.-L., Quayle, B., Howard, S., 2007. A Project for Monitoring Trends in Burn Severity. fire ecol 3, 3–21. https://doi.org/10.4996/fireecology.0301003

Faustini, A., Stafoggia, M., Colais, P., Berti, G., Bisanti, L., Cadum, E., Cernigliaro, A., Mallone, S., Scarnato, C., Forastiere, F., 2013. Air pollution and multiple acute respiratory outcomes. European Respiratory Journal 42, 304–313. https://doi.org/10.1183/09031936.00128712

Feng, X., Mickley, L.J., Bell, M.L., Liu, T., Fisher, J.A., Val Martin, M., 2024a. Improved estimates of smoke exposure during Australia fire seasons: importance of quantifying plume injection heights. Atmospheric Chemistry and Physics 24, 2985–3007. https://doi.org/10.5194/acp-24-2985-2024

Feng, X., Mickley, L. J., Kaplan, J. O., Kelp, M., Li, Y., & Liu, T. 2024b. Large role of anthropogenic climate change in driving smoke exposure across the western United States from 1992 to 2020 (arXiv:2412.03733). arXiv. https://doi.org/10.48550/arXiv.2412.03733

Ferner, C., Meriam, E., 2022. Be Wildfire Aware with this new application. ArcGIS Blog. URL https://www.esri.com/arcgis-blog/products/arcgis-living-atlas/public-safety/wildfire-aware/ (accessed 11.16.24).

Ford, B., Val Martin, M., Zelasky, S.E., Fischer, E.V., Anenberg, S.C., Heald, C.L., Pierce, J.R., 2018. Future Fire Impacts on Smoke Concentrations, Visibility, and Health in the Contiguous United States. GeoHealth 2, 229–247. https://doi.org/10.1029/2018GH000144

Giglio, L., Boschetti, L., Roy, D.P., Humber, M.L., Justice, C.O., 2018. The Collection 6 MODIS burned area mapping algorithm and product. Remote Sensing of Environment 217, 72–85. https://doi.org/10.1016/j.rse.2018.08.005

Giglio, L., Schroeder, W., Justice, C.O., 2016. The collection 6 MODIS active fire detection algorithm and fire products. Remote Sensing of Environment 178, 31–41. https://doi.org/10.1016/j.rse.2016.02.054

Gorelick, N., Hancher, M., Dixon, M., Ilyushchenko, S., Thau, D., Moore, R., 2017. Google Earth Engine: Planetary-scale geospatial analysis for everyone. Remote Sensing of

Environment, Big Remotely Sensed Data: tools, applications and experiences 202, 18–27. https://doi.org/10.1016/j.rse.2017.06.031
Guo, Y., Wang, J., Ge, Y., Zhou, C., 2024. Global expansion of wildland-urban interface intensifies human exposure to wildfire risk in the 21st century. Science Advances 10, eado9587. https://doi.org/10.1126/sciadv.ado9587
Henze, D.K., Hakami, A., Seinfeld, J.H., 2007. Development of the adjoint of GEOS-Chem. Atmospheric Chemistry and Physics 7, 2413–2433. https://doi.org/10.5194/acp-7-2413-2007
Hersbach, H., Bell, B., Berrisford, P., Hirahara, S., Horányi, A., Muñoz-Sabater, J., Nicolas, J., Peubey, C., Radu, R., Schepers, D., Simmons, A., Soci, C., Abdalla, S., Abellan, X., Balsamo, G., Bechtold, P., Biavati, G., Bidlot, J., Bonavita, M., De Chiara, G., Dahlgren, P., Dee, D., Diamantakis, M., Dragani, R., Flemming, J., Forbes, R., Fuentes, M., Geer, A., Haimberger, L., Healy, S., Hogan, R.J., Hólm, E., Janisková, M., Keeley, S., Laloyaux, P., Lopez, P., Lupu, C., Radnoti, G., de Rosnay, P., Rozum, I., Vamborg, F., Villaume, S., Thépaut, J.-N., 2020. The ERA5 global reanalysis. Quarterly Journal of the Royal Meteorological Society 146, 1999–2049. https://doi.org/10.1002/qj.3803
Hessburg, P.F., Churchill, D.J., Larson, A.J., Haugo, R.D., Miller, C., Spies, T.A., North, M.P., Povak, N.A., Belote, R.T., Singleton, P.H., Gaines, W.L., Keane, R.E., Aplet, G.H., Stephens, S.L., Morgan, P., Bisson, P.A., Rieman, B.E., Salter, R.B., Reeves, G.H., 2015. Restoring fire-prone Inland Pacific landscapes: seven core principles. Landscape Ecology 30, 1805–1835. https://doi.org/10.1007/s10980-015-0218-0
Institute for Health Metrics and Evaluation (IHME). 2020. Global Burden of Disease Study 2019 (GBD 2019) Data Resources. Retrieved from https://ghdx.healthdata.org/gbd-2019
Jaffe, D.A., O'Neill, S.M., Larkin, N.K., Holder, A.L., Peterson, D.L., Halofsky, J.E., Rappold, A.G., 2020. Wildfire and prescribed burning impacts on air quality in the United States. Journal of the Air & Waste Management Association 70, 583–615. https://doi.org/10.1080/10962247.2020.1749731
Kelp, M., Burke, M., Qiu, M., Higuera-Mendieta, I., Liu, T., Diffenbaugh, N.S., 2024. Efficacy of Recent Prescribed Burning and Land Management on Wildfire Burn Severity and Smoke Emissions in the Western United States.
Kelp, M.M., Carroll, M.C., Liu, T., Yantosca, R.M., Hockenberry, H.E., Mickley, L.J., 2023. Prescribed Burns as a Tool to Mitigate Future Wildfire Smoke Exposure: Lessons for States and Rural Environmental Justice Communities. Earth's Future 11, e2022EF003468. https://doi.org/10.1029/2022EF003468
Kim, P.S., Jacob, D.J., Mickley, L.J., Koplitz, S.N., Marlier, M.E., DeFries, R.S., Myers, S.S., Chew, B.N., Mao, Y.H., 2015. Sensitivity of population smoke exposure to fire locations in Equatorial Asia. Atmospheric Environment 102, 11–17. https://doi.org/10.1016/j.atmosenv.2014.09.045
Koplitz, S.N., Mickley, L.J., Marlier, M.E., Buonocore, J.J., Kim, P.S., Liu, T., Sulprizio, M.P., DeFries, R.S., Jacob, D.J., Schwartz, J., Pongsiri, M., Myers, S.S., 2016. Public health impacts of the severe haze in Equatorial Asia in September–October 2015: demonstration of a new framework for informing fire management strategies to reduce downwind smoke exposure. Environ. Res. Lett. 11, 094023. https://doi.org/10.1088/1748-9326/11/9/094023

Kramer, S.J., Huang, S., McClure, C.D., Chaveste, M.R., Lurmann, F., 2023. Projected smoke impacts from increased prescribed fire activity in California's high wildfire risk landscape. Atmospheric Environment 311, 119993. https://doi.org/10.1016/j.atmosenv.2023.119993

La Puma, I.P., ed., 2023, LANDFIRE technical documentation: U.S. Geological Survey Open-File Report 2023–1045, 103 p., https://doi.org/10.3133/ofr20231045.

Larkin, N.K., O'Neill, S.M., Solomon, R., Raffuse, S., Strand, T., Sullivan, D., Krull, C., Rorig, M., Peterson, J., Ferguson, S.A., 2009. The BlueSky smoke modeling framework. International Journal of Wildland Fire 18(8), 906–920. https://doi.org/10.1071/WF07086

Liu, J.C., Wilson, A., Mickley, L.J., Dominici, F., Ebisu, K., Wang, Y., Sulprizio, M.P., Peng, R.D., Yue, X., Son, J.-Y., Anderson, G.B., Bell, M.L., 2017. Wildfire-specific Fine Particulate Matter and Risk of Hospital Admissions in Urban and Rural Counties. Epidemiology 28, 77–85. https://doi.org/10.1097/EDE.0000000000000556

Liu, T., Panday, F.M., Caine, M.C., Kelp, M., Pendergrass, D.C., Mickley, L.J., Ellicott, E.A., Marlier, M.E., Ahmadov, R., James, E.P., 2024. Is the smoke aloft? Caveats regarding the use of the Hazard Mapping System (HMS) smoke product as a proxy for surface smoke presence across the United States. Int. J. Wildland Fire 33. https://doi.org/10.1071/WF23148

Magzamen, S., Gan, R.W., Liu, J., O'Dell, K., Ford, B., Berg, K., Bol, K., Wilson, A., Fischer, E.V., Pierce, J.R., 2021. Differential Cardiopulmonary Health Impacts of Local and Long-Range Transport of Wildfire Smoke. GeoHealth 5, e2020GH000330. https://doi.org/10.1029/2020GH000330

Marlier, M.E., Liu, T., Yu, K., Buonocore, J.J., Koplitz, S.N., DeFries, R.S., Mickley, L.J., Jacob, D.J., Schwartz, J., Wardhana, B.S., Myers, S.S., 2019. Fires, Smoke Exposure, and Public Health: An Integrative Framework to Maximize Health Benefits From Peatland Restoration. GeoHealth 3, 178–189. https://doi.org/10.1029/2019GH000191

McClure, C.D., Jaffe, D.A., 2018. US particulate matter air quality improves except in wildfire-prone areas. Proc Natl Acad Sci U S A 115, 7901–7906. https://doi.org/10.1073/pnas.1804353115

O'Dell, K., Bilsback, K., Ford, B., Martenies, S.E., Magzamen, S., Fischer, E.V., Pierce, J.R., 2021. Estimated Mortality and Morbidity Attributable to Smoke Plumes in the United States: Not Just a Western US Problem. GeoHealth 5, e2021GH000457. https://doi.org/10.1029/2021GH000457

O'Dell, K., Ford, B., Fischer, E.V., Pierce, J.R., 2019. Contribution of Wildland-Fire Smoke to US PM2.5 and Its Influence on Recent Trends. Environ. Sci. Technol. 53, 1797–1804. https://doi.org/10.1021/acs.est.8b05430

Picotte, J.J., Bhattarai, K., Howard, D., Lecker, J., Epting, J., Quayle, B., Benson, N., Nelson, K., 2020. Changes to the Monitoring Trends in Burn Severity program mapping production procedures and data products. Fire Ecology 16, 16. https://doi.org/10.1186/s42408-020-00076-y

Prichard, S.J., Karau, E.C., Ottmar, R.D., Kennedy, M.C., Cronan, J.B., Wright, C.S., Keane, R.E., 2014. Evaluation of the CONSUME and FOFEM fuel consumption models in pine and mixed hardwood forests of the eastern United States. Can. J. For. Res. 44, 784–795. https://doi.org/10.1139/cjfr-2013-0499

Qiu, M., Kelp, M., Heft-Neal, S., Jin, X., Gould, C., Tong, D., Burke, M., 2024. Evaluating estimation methods for wildfire smoke and their implications for assessing health effects.

Randerson, J.T., Chen, Y., van der Werf, G.R., Rogers, B.M., Morton, D.C., 2012. Global burned area and biomass burning emissions from small fires. Journal of Geophysical Research: Biogeosciences 117. https://doi.org/10.1029/2012JG002128

Reid, C.E., Brauer, M., Johnston, F.H., Jerrett, M., Balmes, J.R., Elliott, C.T., 2016. Critical Review of Health Impacts of Wildfire Smoke Exposure. Environmental Health Perspectives 124, 1334–1343. https://doi.org/10.1289/ehp.1409277

Schollaert, C.L., Marlier, M.E., Marshall, J.D., Spector, J.T., Busch Isaksen, T., 2024. Exposure to Smoke From Wildfire, Prescribed, and Agricultural Burns Among At-Risk Populations Across Washington, Oregon, and California. Geohealth 8, e2023GH000961. https://doi.org/10.1029/2023GH000961

Silva, F.R. y, O'Connor, C.D., Thompson, M.P., Martinez, J.R.M., Calkin, D.E., 2020. Modelling suppression difficulty: Current and future applications. International Journal of Wildland Fire. doi: 10.1071/WF19042. https://doi.org/10.1071/WF19042

Stephens, S.L., Collins, B.M., Fettig, C.J., Finney, M.A., Hoffman, C.M., Knapp, E.E., North, M.P., Safford, H., Wayman, R.B., 2018. Drought, Tree Mortality, and Wildfire in Forests Adapted to Frequent Fire. BioScience 68, 77–88. https://doi.org/10.1093/biosci/bix146

Sulla-Menashe, D., Gray, J.M., Abercrombie, S.P., Friedl, M.A., 2019. Hierarchical mapping of annual global land cover 2001 to present: The MODIS Collection 6 Land Cover product. Remote Sensing of Environment 222, 183–194. https://doi.org/10.1016/j.rse.2018.12.013

Tuet, W.Y., Liu, F., de Oliveira Alves, N., Fok, S., Artaxo, P., Vasconcellos, P., Champion, J.A., Ng, N.L., 2019. Chemical Oxidative Potential and Cellular Oxidative Stress from Open Biomass Burning Aerosol. Environ. Sci. Technol. Lett. 6, 126–132. https://doi.org/10.1021/acs.estlett.9b00060

Turpin, B.J., Lim, H.-J., 2001. Species Contributions to PM2.5 Mass Concentrations: Revisiting Common Assumptions for Estimating Organic Mass. Aerosol Science and Technology 35, 602–610. https://doi.org/10.1080/02786820119445

U. S. Department of Agriculture, 2023. National Prescirbed Fire Resource Mobilization Strategy.

U.S. EPA. 2021. Comparative Assessment of the Impacts of Prescribed Fire Versus Wildfire (CAIF): A Case Study in the Western U.S. U.S. Environmental Protection Agency, Washington, DC, EPA/600/R-21/197, 2021.

van der Werf, G.R., Randerson, J.T., Giglio, L., van Leeuwen, T.T., Chen, Y., Rogers, B.M., Mu, M., van Marle, M.J.E., Morton, D.C., Collatz, G.J., Yokelson, R.J., Kasibhatla, P.S., 2017. Global fire emissions estimates during 1997–2016. Earth System Science Data 9, 697–720. https://doi.org/10.5194/essd-9-697-2017

Verma, V., Fang, T., Xu, L., Peltier, R.E., Russell, A.G., Ng, N.L., Weber, R.J., 2015. Organic Aerosols Associated with the Generation of Reactive Oxygen Species (ROS) by Water-Soluble PM2.5. Environ. Sci. Technol. 49, 4646–4656. https://doi.org/10.1021/es505577w

Vodonos, A., Awad, Y.A., Schwartz, J., 2018. The concentration-response between long-term PM2.5 exposure and mortality; A meta-regression approach. Environmental Research 166, 677–689. https://doi.org/10.1016/j.envres.2018.06.021

Vohra, K., Vodonos, A., Schwartz, J., Marais, E.A., Sulprizio, M.P., Mickley, L.J., 2021. Global mortality from outdoor fine particle pollution generated by fossil fuel combustion: Results from GEOS-Chem. Environmental Research 195, 110754. https://doi.org/10.1016/j.envres.2021.110754

Wang, Q., Jacob, D.J., Fisher, J.A., Mao, J., Leibensperger, E.M., Carouge, C.C., Le Sager, P., Kondo, Y., Jimenez, J.L., Cubison, M.J., Doherty, S.J., 2011. Sources of carbonaceous aerosols and deposited black carbon in the Arctic in winter-spring: implications for radiative forcing. Atmospheric Chemistry and Physics 11, 12453–12473. https://doi.org/10.5194/acp-11-12453-2011

Williams, A.P., Cook, E.R., Smerdon, J.E., Cook, B.I., Abatzoglou, J.T., Bolles, K., Baek, S.H., Badger, A.M., Livneh, B., 2020. Large contribution from anthropogenic warming to an emerging North American megadrought. Science 368, 314–318. https://doi.org/10.1126/science.aaz9600

Wu, Y., Cordero, L., Gross, B., Moshary, F., Ahmed, S., 2012. Smoke plume optical properties and transport observed by a multi-wavelength lidar, sunphotometer and satellite. Atmospheric Environment 63, 32–42. https://doi.org/10.1016/j.atmosenv.2012.09.016

Yitshak-Sade, M., Kloog, I., Schwartz, J.D., Novack, V., Erez, O., Just, A.C., 2021. The effect of prenatal temperature and PM2.5 exposure on birthweight: Weekly windows of exposure throughout the pregnancy. Environment International 155, 106588. https://doi.org/10.1016/j.envint.2021.106588

Yu, M., Zhang, S., Ning, H., Li, Z., Zhang, K., 2024. Assessing the 2023 Canadian wildfire smoke impact in Northeastern US: Air quality, exposure and environmental justice. Science of The Total Environment 926, 171853. https://doi.org/10.1016/j.scitotenv.2024.171853

Zhou, X., Josey, K., Kamareddine, L., Caine, M.C., Liu, T., Mickley, L.J., Cooper, M., Dominici, F., 2021. Excess of COVID-19 cases and deaths due to fine particulate matter exposure during the 2020 wildfires in the United States. Science Advances 7, eabi8789. https://doi.org/10.1126/sciadv.abi8789

938 **Supplemental Information**

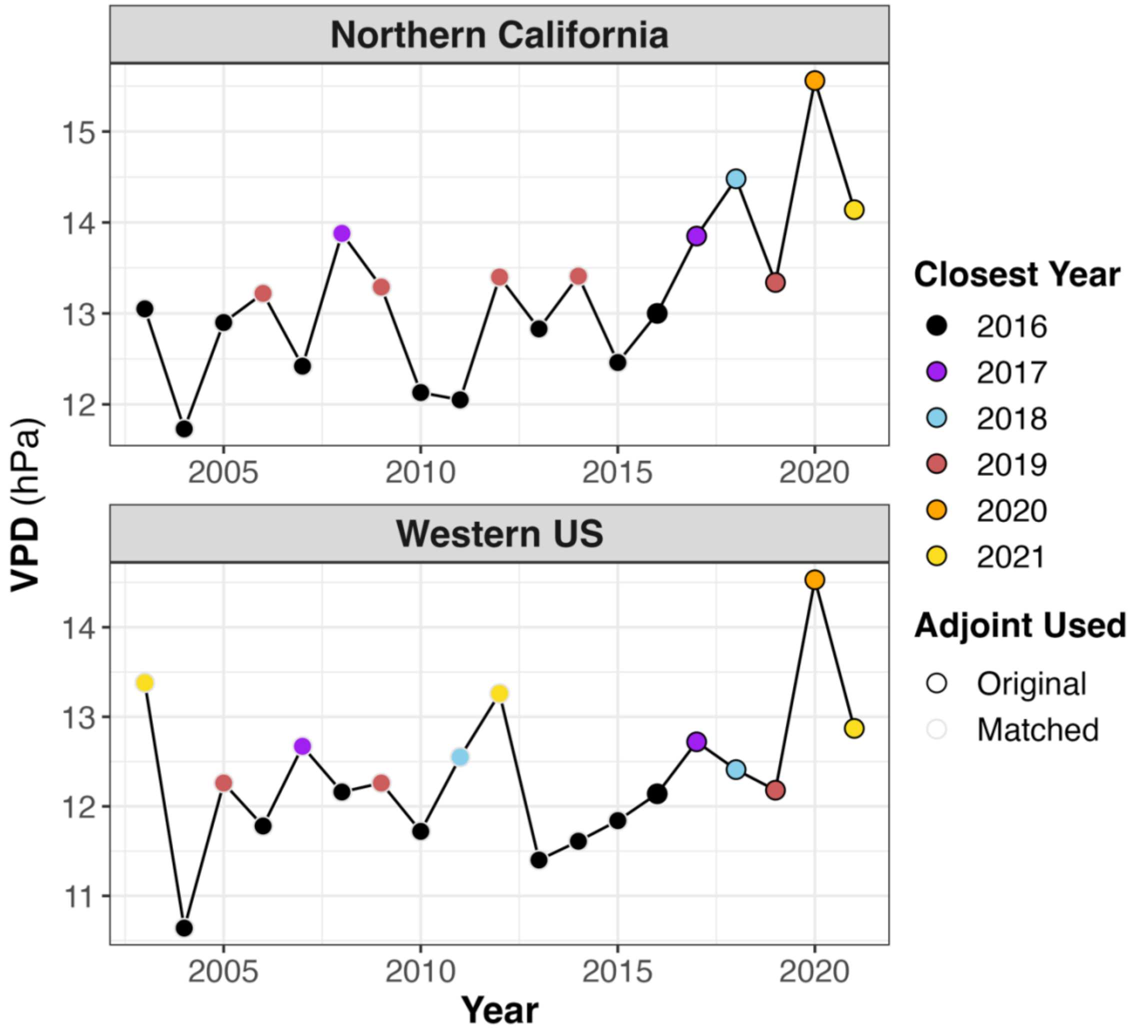

939
940 **Figure S1. Matching GOES-Chem adjoint sensitivities based on the average vapor pressure**
941 **deficit (VPD) by region.** GEOS-Chem adjoint sensitivities for receptors are available for a subset
942 of years, from 2016-2021. The average fire season (Jul-Nov) VPD is shown for Northern
943 California and the western US from 2003-2021. The filled-in colors represent the matched year
944 according to the closest VPD, and the border colors represent whether the original or matched
945 adjoint sensitivities are used.

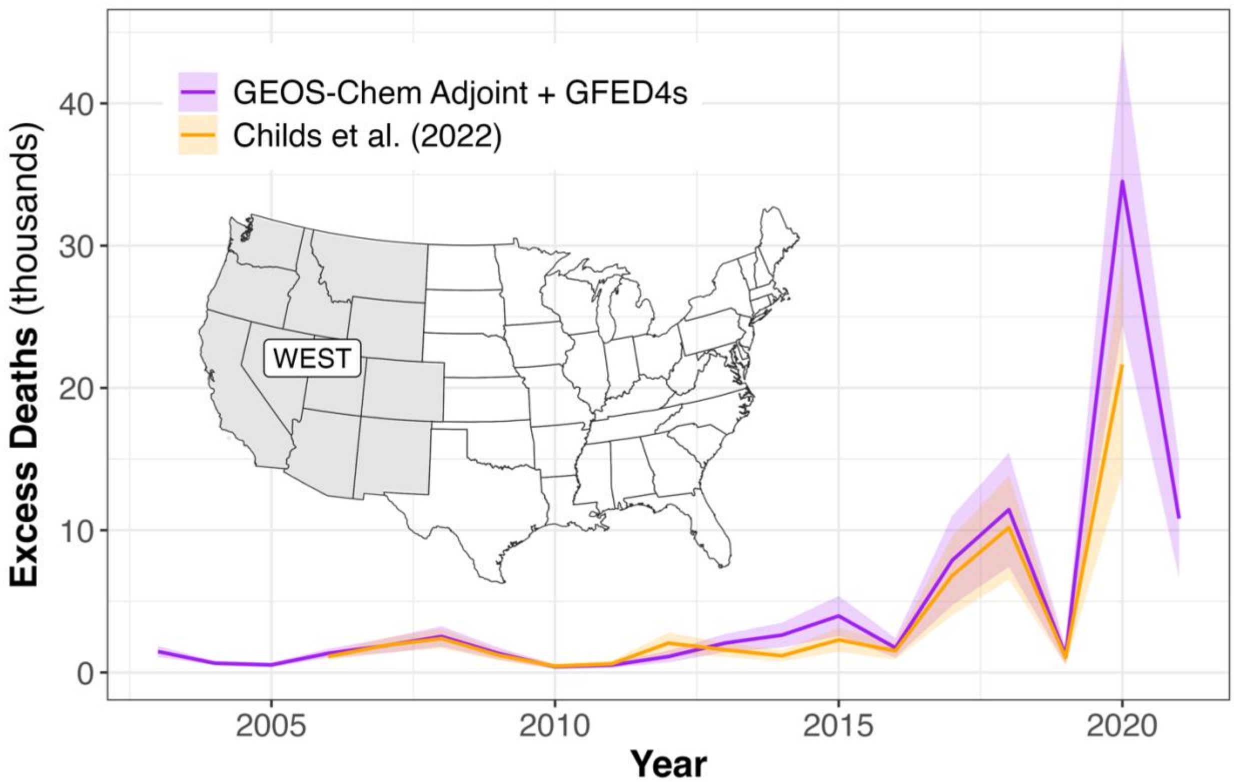

Figure S2. Excess mortality attributable to smoke $PM_{2.5}$ exposure from western US fires in the western US. The GEOS-Chem estimates contain only emissions in the western US, with adjoint sensitivities for a receptor covering all states in the western US. The Childs et al. (2022) data consider all smoke-related $PM_{2.5}$, regardless of source, and are population-weighted for smoke exposure in the western US. The GEOS-Chem estimates rely on GFED4s fire emissions and GEOS-FP meteorology, while Childs et al. (2022) uses a machine learning-based approach with inputs including surface monitor $PM_{2.5}$, satellite-based smoke delineation, and modeled atmospheric transport trajectories. Excess deaths are calculated using the CRF in Vodonos et al. (2018) (see Section 2.3). The shaded areas represent the 95% confidence interval for the excess mortality estimates based on uncertainties in the CRF.

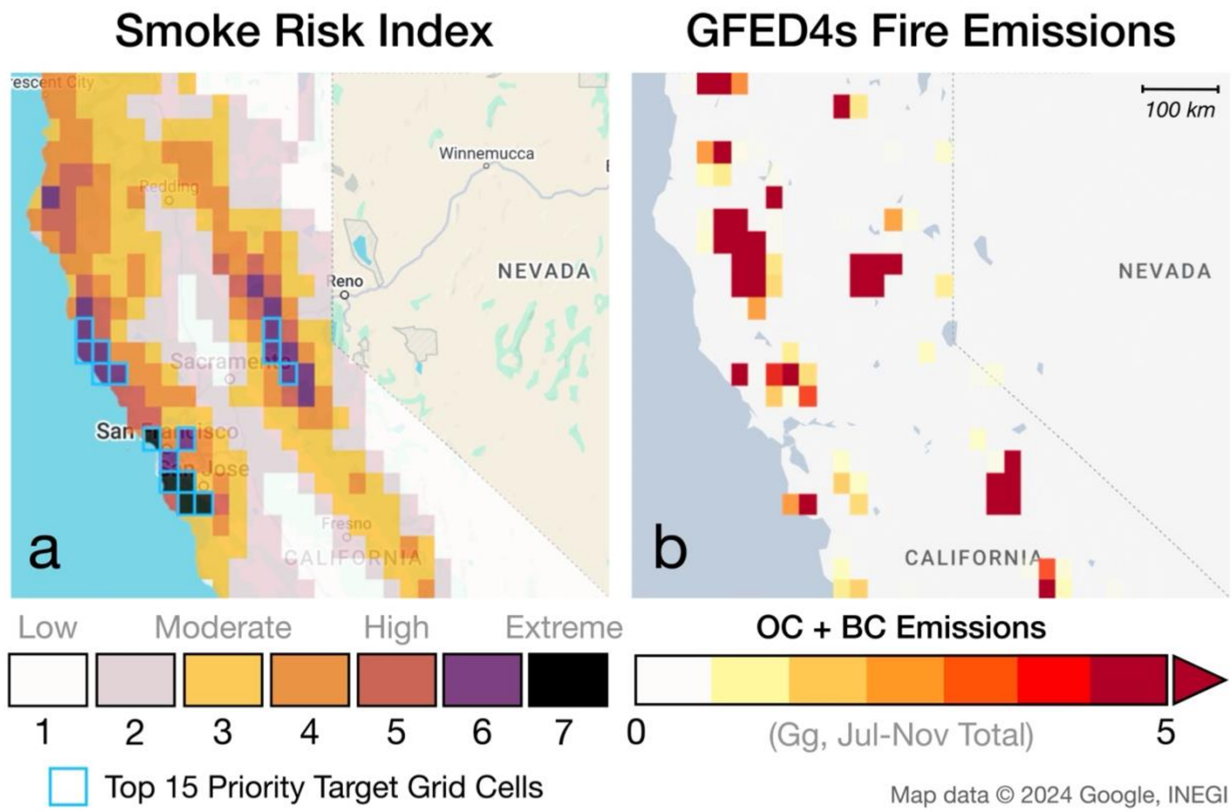

Figure S3. Smoke risk index and historical GFED4s fire emissions in Northern California in 2020. (*a*) Same as Figure 3a, the smoke risk index for the Northern California receptor in the baseline scenario; (*b*) GFED4s fire emissions from July to November 2020. The background map data are from © 2024 Google, INEGI, rendered on Google Earth Engine Apps.

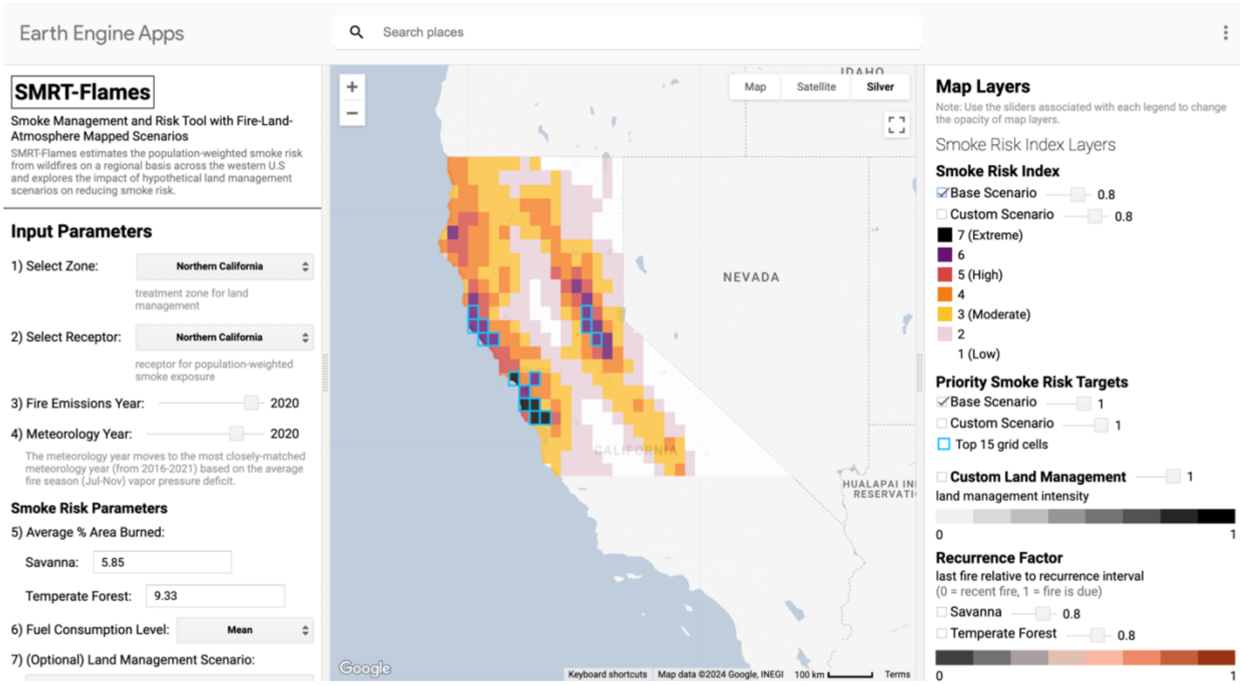

Figure S4. Screenshot of SMRT-Flames on Google Earth Engine Apps. The left panel shows the options for the input parameters. Once a scenario is submitted, charts are displayed below the control panel. The middle panel displays the map layers, and the right panel displays the legends and controls for the map layers. The background map data are from © 2024 Google, INEGI, rendered on Google Earth Engine Apps.